Title

Gd3+ and Eu2+ local environment in Ca1–x Eux B6 (0.0001 ≤ x ≤ 0.30) and Ca1–x Gdx B6 (0.0001 ≤ x ≤ 0.01)

Journal
physica status solidi (a) – applications and materials science, 203(7)

ISSN
1862-6300

Authors

Urbano, RR
Pagliuso, PG
Rettori, C
et al.

Publication Date
2006-05-01

DOI
10.1002/pssa.200563125

phys. stat. sol. (a) **203**, No. 7, 1550–1555 (2006) / **DOI** 10.1002/pssa.200563125

Gd^{3+} and Eu^{2+} local environment in $Ca_{1-x}Eu_xB_6$ ($0.0001 \le x \le 0.30$) and $Ca_{1-x}Gd_xB_6$ ($0.0001 \le x \le 0.01$)

R. R. Urbano[*, 1], **P. G. Pagliuso**[1], **C. Rettori**[**, 1], **P. Schlottmann**[2, 3], **Z. Fisk**[4], **B. Chapler**[5], and **S. B. Oseroff**[5]

[1] Instituto de Física “Gleb Wataghin”, UNICAMP, Campinas-SP 13083-970, Brazil
[2] Department of Physics, Florida State University, Tallahassee FL 32306, USA
[3] National High Magnetic Field Laboratory, Florida State University, Tallahassee FL 32306, USA
[4] UC Davis, Physics Department, CA 95616, USA
[5] San Diego State University, San Diego, CA 92182, USA

Received 5 July 2005, revised 22 February 2006, accepted 7 March 2006

PACS 71.70.Ch, 75.50.Pp, 76.30.Kg

Local environment of Gd^{3+} and Eu^{2+} $4f^7$ ions, $S = 7/2$, in $Ca_{1-x}Eu_xB_6$ ($0.0001 \le x \le 0.30$) and $Ca_xGd_xB_6$ ($0.0001 \le x \le 0.01$) is investigated by means of electron spin resonance (ESR). For $x \le 0.001$ the spectra show resolved fine structures due to the cubic crystal electric field and, in the case of Eu, the hyperfine structure due to the nuclear hyperfine field is also observed. The resonances have Lorentzian line shape, indicating insulating host for the Gd^{3+} and Eu^{2+} ions. As x increases, the ESR lines broaden due to local distortions caused by the Ca/Gd,Eu ions substitution. For Gd ($x \approx 0.001$) and Eu ($x \approx 0.02$), the spectra present superposition of Lorentzian and Dysonian resonances, suggesting a coexistence of insulating and metallic hosts for the Gd^{3+} and Eu^{2+} ions. The Gd^{3+} and Eu^{2+} fine structures are still observable up to $x \approx 0.003$ for Gd and $x \approx 0.15$ for Eu. For larger values of x the fine and hyperfine structures are no longer observed, the line width increases, and the line shape becomes pure Dysonian anticipating the metallic and semimetallic character of GdB_6 and EuB_6, respectively. These results clearly show that in the low concentration regime the $Ca_{1-x}R_xB_6$ (R = Gd, Eu) systems are intrinsically inhomogeneous. No evidence of weak ferromagnetism (WF) was found in the ESR spectra of either metallic or insulating phases of these compounds, suggesting that, if WF is present in these materials, the Gd^{3+} and Eu^{2+} $4f^7$-electrons are shielded from the WF field.

1 Introduction

The simple cubic system (space group 221, Pm3m) of $Ca_{1-x}R_xB_6$ (R = rare-earths, specially La) has become the focus of extensive scientific investigations since the reported weak-ferromagnetism (WF) at high-temperature $T_c \sim 600-800$ K in these materials by Young et al. [1]. Over the last few years, enormous efforts were devoted, both, theoretically [2–8] and experimentally [1, 9–17] to establish the origin of this WF in $Ca_{1-x}La_xB_6$ and its relationship with the actual conducting nature of R doped CaB_6. However, the nature of the WF of the parent compound CaB_6 is still controversial. Studies of the de Haas–van Alphen effect [10, 11] the plasma edge in optical spectroscopy [12, 13] and some electrical resistivity measurements [18] support a semimetallic character for CaB_6 whereas NMR [14] thermopower [16] angle-resolved photoemission (ARPES) [15] and a different set of resistivity measurements [12, 17]

---

[*] Corresponding author: e-mail: urbano@ifi.unicamp.br, Phone: +55 019 3788 5501, Fax: +55 019 3788 5501
[**] e-mail: rettori@ifi.unicamp.br

suggest that CaB_6 is a well defined semiconductor. High-resolution ARPES by Souma et al. [18] revealed an energy gap of about 1 eV between the valence and conduction bands and a carrier density of the order of 5×10^{19} cm^{-3} for their CaB_6 single crystals. Vonlanthen et al. [12] reported that, depending on the crystal growth method, undoped CaB_6 could also show WF. They argue that self-doping attributed to defects might occur. Terashima et al. [19] reported strongly sample dependent data for $Ca_{0.995}La_{0.005}B_6$ and, lately, doubts about the intrinsic nature of the WF in these systems were raised [20]. It has been argued that CaB_6 is a ~1 eV-gap semiconductor and that the intrinsic WF could be hidden by the FM of Fe and Ni impurities at the surface of the crystals [21].

The electronic configuration of Eu^{2+} ions ($4f^7$, $S = 7/2$) is identical to that of the Gd^{3+} ions. However, the effect of Gd^{3+} and Eu^{2+} doping in CaB_6 is expected to be quite different since Eu^{2+} has the same valence as Ca^{2+}, while Gd^{3+} delivers an extra electron to the system creating a hydrogen-like donor state with large Bohr radius. The insulator to metal transition should be then reached when the Gd donor bound-states overlap and start to form a percolative network. Since not all Gd-sites participate in this network, a coexistence of metallic and insulating phases may be expected for Gd concentrations of about 1000 ppm. The substitution of Ca^{2+} by Eu^{2+} impurities does not yield a donor bound state. Instead, the broken translational invariance of the lattice introduces a localized split-off state from the valence/conduction band. The energy of such state lies in the gap of the semiconductor and its spatial extension is of the order of one unit cell. Thus an impurity band for Eu^{2+} only forms at much higher concentrations than for Gd^{3+}, as it is indeed observed in the experiments that we will show below.

Therefore, an ESR study, probing the local Gd^{3+} and Eu^{2+} environment in $Ca_{1-x}R_xB_6$ (R = Gd, Eu), is of great interest to understand the magnetic/non-magnetic and metallic/non-metallic properties of these materials. In this work we present a systematic Gd^{3+} and Eu^{2+} ESR study of $Ca_{1-x}R_xB_6$ single crystals ($0.0001 \le x \le 0.01$ for Gd and $0.003 \le x \le 0.30$ for Eu). Preliminary X-band data in some of these samples were already presented previously [22] and a complete set of data for the case of Eu^{2+} was reported in Ref. [23]. For EuB_6 ($x = 1.00$) Urbano et al. [24] have recently attributed the broad line width observed in their ESR experiments to a spin-flip scattering relaxation process due to the exchange interaction between the Eu^{2+} $4f^7$ and conduction electrons. As a consequence, the observed field, temperature, and angular dependence of the ESR line width could be associated with the Fermi surface of the conduction electrons and the formation of magnetic polarons.

2 Experiments

Single crystals of $Ca_{1-x}R_xB_6$ (R = Gd, Eu; $0.0001 \le x \le 0.01$ for Gd and $0.003 \le x \le 0.30$ for Eu) were grown as described in Ref. [1]. The structure and phase purity were checked by X-ray powder diffraction and the crystal orientation determined by Laue X-ray diffraction. Most of the ESR experiments were done in $\sim 1 \times 0.5 \times 0.3$ mm^3 single crystals in a Bruker spectrometer using a X-band (9.479 GHz) TE_{102} room-T cavity coupled to a T-controller using a helium gas flux system for $4.2 \le T \le 300$ K. $M(T, H)$ measurements for $2 \le T \le 300$ K were taken in a Quantum Design SQUID-RSO dc-magnetometer. The Gd^{3+} and Eu^{2+} concentrations were obtained from Curie–Weiss fits of the susceptibility data.

3 Experimental results

Figure 1 presents the X-band ESR spectra of Eu^{2+} in $Ca_{1-x}Eu_xB_6$ single crystals at room-T and $H \parallel [001]$. For $x = 0.003$ the spectrum shows the fine and hyperfine structures corresponding to seven groups ($4f^7$, $S = 7/2$) of twelve hyperfine resonances due to the $^{151}Eu^{2+}$ (47.8%; $I = 5/2$) and $^{153}Eu^{2+}$ (52.2%; $I = 5/2$) isotopes [25]. The line shape of the individual resonances is Lorentzian as expected for Eu^{2+} ions in an insulating host. The observed isotropic g-value (1.988(4)) and anisotropy of the fine structure confirms that the Eu^{2+} local symmetry is cubic. These results are in agreement with the data reported by Urbano et al. [9]. For $x = 0.023$, 0.07, 0.15 and 0.30 the data show that the individual resonances and the spectra, as a whole, become broader as x increases. Nonetheless, the Eu^{2+} resolved fine structure is still observed up to Eu concentrations of $x \approx 0.15$.

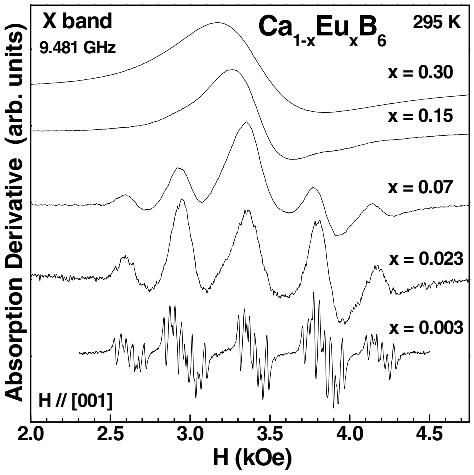

Fig. 1 Experimental X-band ESR spectra of Eu^{2+} in $Ca_{1-x}Eu_xB_6$ single crystals for $0.0003 \le x \le 0.30$ at room-T and $H \parallel [001]$.

Figure 2 displays the X-band ESR spectra at room-T for the $x = 0.023$, 0.07, and 0.30 samples of Fig. 1. The experimental spectra for $x = 0.023$ and 0.07 were simulated (S) by the superposition of two different Eu^{2+} ESR spectra: a spectrum with resolved fine structure of Lorentzian resonances (*fsL*) corresponding to Eu^{2+} ions in an insulating host and a single Dysonian (D) resonance associated to Eu^{2+} ions in a metallic phase [26]. For $x = 0.30$ the spectrum can be simulated with just the D resonance. These results unambiguously confirm, for the Eu^{2+} ions in $Ca_{1-x}Eu_xB_6$, the coexistence of two different phases in the concentration range of $0.023 \le x \le 0.15$.

Figure 3 presents the X-band ESR spectra of Gd^{3+} in $Ca_{1-x}Gd_xB_6$ single crystals at 4.2 K and $H \parallel [001]$. For $x = 0.0001$ the spectrum shows the seven resonances ($4f^7$, $S = 7/2$) corresponding to the fine structure [25]. The line shape of the individual resonances is Lorentzian indicating an insulating host for the Gd^{3+} ions. The observed isotropic g-value (1.993(4)) and anisotropy of the fine structure confirms that the Gd^{3+} local symmetry is cubic. These results are in agreement with the data reported by Urbano et al. [9]. For $x = 0.0013$ and 0.003 the data show that the Gd^{3+} resolved fine structure is still observed up to Gd concentrations of $x \approx 0.003$. This is in contrast to Eu^{2+} in $Ca_{1-x}Eu_xB_6$, where Eu concentration larger than $x \approx 0.15$ was necessary to collapse the entire spectrum into a single metallic line [9].

Figure 4 displays the X-band spectra at 4.2 K for the $x = 0.0013$ and 0.01 samples of Fig. 3. The experimental spectra were simulated (S) by the superposition of two different Gd^{3+} ESR spectra: a spectrum with resolved *fsL* resonances corresponding to Gd^{3+} ions in an insulating host and a single D resonance associated to Gd^{3+} ions in a metallic phase. For $x = 0.01$ the spectrum can be simulated with just a single

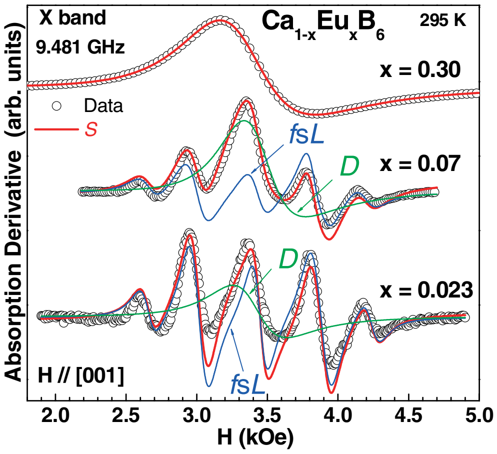

Fig. 2 (online colour at: www.pss-a.com) X-band ESR spectra for $x = 0.023$, $x = 0.07$ and $x = 0.30$ at room-T and $H \parallel [001]$. Open symbols are experimental data. The *fsL* (blue) spectrum corresponds to the 7 resonances in a cubic insulating phase. The single D resonance corresponds to the metallic phase. For $x = 0.023$ and $x = 0.07$ the simulations S (red) of the data correspond to the superposition of *fsL* and D. For $x = 0.30$ S is given by a single D resonance (see text).

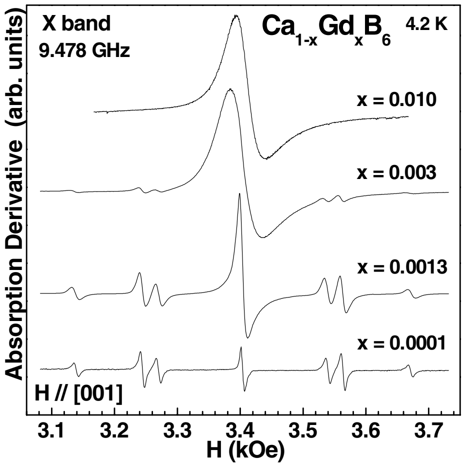

Fig. 3 Experimental X-band ESR spectra of Gd^{3+} in $Ca_{1-x}Gd_xB_6$ single crystals for $0.0001 \le x \le 0.01$ at 4.2 K and $H \parallel [001]$.

D resonance. These results unambiguously confirm, for the Gd^{3+} ions in $Ca_{1-x}Gd_xB_6$, the coexistence of two different phases in a very narrow concentration range of $0.001 \le x \le 0.003$.

4 Analysis and discussion

The spectra of Gd^{3+} and Eu^{2+} in $Ca_{1-x}R_xB_6$ (R = Gd, Eu) presented in this paper show three different concentration regimes. For low R concentrations the resonance line shapes are Lorentzian, therefore, the Gd^{3+} and Eu^{2+} environment is insulating and, as a consequence of the relatively slow spin-lattice relaxation, the fine and hyperfine (Eu^{2+}) structures are fully resolved. From the isotropic *g*-value and anisotropy of the fine structure (not shown in this work) it is inferred that the Gd^{3+} and Eu^{2+} local symmetry is cubic. For intermediate R concentrations the ESR spectra present a superposition of a resolved *fsL* structure and a single *D* resonance (see Figs. 2 and 4). In this regime the ESR line shape begins to show a Dysonian shape, i.e. it starts to display metallic character (see Figs. 1 and 3). So, the microwave skin depth became comparable with the size of the metallic phase. For higher R concentrations the ESR line shape is pure Dysonian, i.e., there is spin diffusion and the crystal becomes metallic. In this regime the fine and hyperfine structures can no longer be resolved. For Eu^{2+} and $x \le 0.60$, the *g*-value and line width are *T*-independent down to ~20–30 K [23, 24]. The absence, or negligible, *T*-dependence for these parameters assure us, within the experimental error, that above ~30 K there is no direct or indirect magnetic interaction between the R ions in these systems.

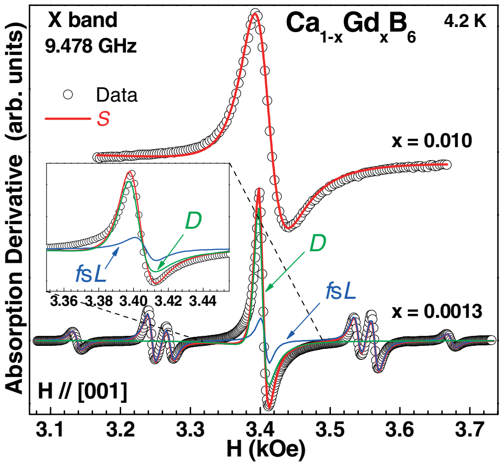

Fig. 4 (online colour at: www.pss-a.com) X-band ESR spectra for $x = 0.0013$ and $x = 0.01$ at 4.2 K and $H \parallel [001]$. Open symbols are experimental data. The *fsL* (blue) spectrum corresponds to the 7 resonances in a cubic insulating phase. The single *D* (green) resonance corresponds to the metallic phase. For $x = 0.0013$ the simulation *S* (red) of the data corresponds to the superposition of *fsL* and *D*. For $x = 0.01$ *S* is given by a single *D* resonance (see text). The inset is a blow-up of the central part of the spectrum.

In the small x limit for $Ca_{1-x}Eu_xB_6$, each Eu^{2+} represents a charge neutral substitution, which gives rise to a bound state in the gap of the semiconductor, as a consequence of the broken translational invariance. The impurity states are localized within the extension of about one unit cell. As the number of impurity states increases with x, they start to overlap and eventually form a percolative network. The critical concentration for nearest neighbor (nn) site percolation on a simple cubic lattice is $x_c = 0.307$ [27]. The percolation threshold is reduced to $x_c = 0.137$ if next-to-nearest neighbors (nnn) are included, which correspond to neighbors in the [110]-directions. Third neighbors are along the diagonals of the cube, but this direction is blocked for the wave functions because of the large B_6^{2-} anions. Our data clearly indicate a phase separation into an insulating and a metallic phase for concentrations of Gd and Eu above $x = 0.001$ and 0.01, respectively. These values are well bellow the percolation threshold for nn, nnn and next to nnn ($x_c = 0.307$, 0.137, and 0.099). Thus, as previously reported by Wigger et al. [28] for $Eu_{1-x}Ca_xB_6$, from their high resolution transmission electron microscopy data (HRTEM), we have also observed two phases, one of Ca and the other of Eu or Gd rich, in crystals grown in the same way. However, the ESR data indicate that the separation occurs at much lower concentrations than $x \approx 0.27$ as reported by HRTEM. Besides, the presence of a Dysonian line shape indicates that the size of the Eu or Gd rich regions should be of the order of the skin-depth. From the resistivity data of pure EuB_6 and GdB_6 and the ESR data we estimate that the extension of these regions is as large as one micron, in contrast with the 5 to 10 nm observed by HRTEM. This raises the interesting question, of what really constitute these metallic phases observed by ESR. For example, no indication of a FM transition coming from possible EuB_6 "clusters" at $T \approx 15$ K is observed in these samples. In the HRTEM study by Wigger et al. [28] they found that their $x \approx 0.27$ sample presented separated regions rich in Ca^{2+} (insulating) and Eu^{2+} ions (semimetallic). According to these results, we may associate the fsL spectra in Figs. 2 and 4 with regions rich in Ca^{2+} and the D resonance with regions rich in Eu^{2+}. This is actually similar to the case of $Ca_{1-x}Gd_xB_6$ where coexistence of insulating and metallic phases is inferred from the Gd^{3+} ESR spectra, although, at much lower of Gd concentrations (see Figs. 1 and 3).

The data at room-T shows a gradual broadening of the individual Eu^{2+} resonances with increasing x (see Fig. 1). We argue that this cannot be attributed to Eu^{2+}–Eu^{2+} magnetic correlations because the g-value and the line width are T-independent down to ~20–30 K (see above). Thus, the broadening may be attributed to site symmetry breaking due to Ca/Eu substitution. This inhomogeneous broadening is probably responsible for hiding the Eu^{2+} fine and hyperfine structures as x increases. Weak or no T-dependence is expected from this inhomogeneous broadening.

With respect to the controverter scenario about the conducting nature of stoichiometric CaB_6, the Eu^{2+} ESR results in $Ca_{1-x}Eu_xB_6$ for $x \le 0.003$ and those in $Ca_{1-x}Gd_xB_6$ for $x \le 0.001$ [9], revealed an insulating host for the dopants, Eu^{2+} and Gd^{3+}, supporting that pure CaB_6 is a "wide-gap" semiconductor.

Regarding the reported sample dependence for $Ca_{1-x}R_xB_6$, we would like to point out that in our study neither the Eu^{2+} ESR spectra nor the $M(H)$ data in $Ca_{1-x}Eu_xB_6$ were found to be sample dependent. Our $M(H)$ measurements show that all our crystals presented a $WF \le 0.5$ emu/mole, i.e., smaller than for La-doped CaB_6 crystals which were grown using the same method [1, 9]. Furthermore, for $x \ge 0.10$, the WF component became difficult to measure due to the large M of Eu^{2+}. The above results suggest that the WF is probably caused by self-doping or extrinsic impurities which are inherent to the employed materials and crystal growth method. These results are quite different from those observed in the ESR data of Gd-doped CaB_6 where strong sample dependent ESR spectra were reported for concentrations of $x \approx 0.001$–0.002. This is to be attributed to the donor states provided by the Ca/Gd substitution.

5 Conclusions

In summary, we have reported ESR results in $Ca_{1-x}R_xB_6$ for R = Eu, Gd. As a function of the R concentration, an evolution from insulating to a metallic phase is observed from the change in the line shape of the Eu^{2+} and Gd^{3+} ESR spectra. The threshold for the percolative transition between these two regimes is estimated to be at $x \approx 0.14$ for the Eu doped samples, indicating that nnn bound states are already contributing to the percolative network. For an intermediate range of R concentration, coexisting of insulating and metallic phases are observed. Similarly to $Ca_{1-x}Eu_xB_6$ coexistence of insulating and metallic phases was also found in $Ca_{1-x}Gd_xB_6$, however, due to the Gd^{3+} doping extra electron the Dysonian resonance and the percolative interval is found at a much lower level of Gd concentration ($x \approx 0.0015$) than that for the Eu doped crystals.

Acknowledgements The work at UNICAMP was supported by FAPESP and CNPq. The work at the NHMFL by NSF Cooperative Agreement No. DMR-9527035 and the State of Florida. The support by NSF (grants Nos. DMR-0102235 and DMR-0105431) and DOE (grant No. DE-FG02-98ER45797) is also acknowledged.

References

[1] D. P. Young et al., Nature **397**, 412 (1999).
[2] M. E. Zhitomirsky et al., Nature **402**, 251 (1999).
[3] L. Balents and C. M. Varma, Phys. Rev. Lett. **84**, 1264 (2000).
[4] V. Barzykin and L. P. Gor'kov, Phys. Rev. Lett. **84**, 2207 (2000).
[5] T. Jarlborg, Physica B **307**, 291 (2001); Phys. Rev. Lett. **85**, 186 (2000).
[6] D. Ceperley, Nature **397**, 386 (1999).
[7] H. J. Tromp et al., Phys. Rev. Lett. **87**, 16401 (2000).
[8] S. Massidda, A. Continenza, T. M. de Pascale, and R. Monnier, Z. Phys. B, Condens. Matter **102**, 83 (1997).
[9] R. R. Urbano, C. Rettori, G. E. Barberis, M. Torelli, A. Bianchi, Z. Fisk, P. G. Pagliuso, A. Malinowski, M. F. Hundley, J. L. Sarrao, and S. B. Oseroff, Phys. Rev. B **65**, 180407(R) (2002).
[10] T. Moriwaka et al., J. Phys. Soc. Jpn. **70**, 341 (2001).
[11] D. Hall et al., Phys. Rev. B **64**, 233105 (2001).
[12] P. Vonlanthen et al., Phys. Rev. B **62**, 10076 (2000).
[13] H. R. Ott et al., Z. Phys. B **102**, 337 (1997).
[14] J. L. Gavilano et al., Phys. Rev. B **63**, 140410(R) (2001).
[15] K. Giannio et al., J. Phys. Condens. Matter **14**, 1035 (2002).
[16] J. D. Denlinger et al., Phys. Rev. Lett. **89**, 157601 (2002).
[17] Jong-Soo Rhyee, B. K. Cho, and H.-C. Ri, Phys. Rev. B **67**, 125102 (2003).
[18] S. Souma, H. Komatsu, T. Takahashi, R. Kaji, T. Sasaki, Y. Yokoo, and J. Akimitsu, Phys. Rev. Lett. **90**, 027202 (2003).
[19] T. Terashima et al., J. Phys. Soc. Jpn. **69**, 2423 (2000).
[20] K. Matsubayashi, M. Maki, T. Tsuzuki et al., Nature **420**, 143 (2002).
Z. Fisk, Nature **420**, 144 (2002).
[21] M. C. Bennett, J. van Lierop, E. M. Berkeley, J. F. Mansfield, C. Henderson, M. C. Aronson, D. P. Young, A. Bianchi, Z. Fisk, F. Balakirev, and A. Lacerda, Phys. Rev. B **69**, 132407 (2004).
[22] R. R. Urbano, P. G. Pagliuso, J. L. Sarrao, S. B. Oseroff, C. Rettori, A. Bianchi, S. Nakatsuji, and Z. Fisk, J. Magn. Magn. Mater. **272–276** (Suppl. 1), E1659 (2004).
[23] R. R. Urbano, P. G. Pagliuso, C. Rettori, P. Schlottmann, J. L. Sarrao, A. Bianchi, S. Nakatsuji, Z. Fisk, and S. B. Oseroff, Phys. Rev. B **71**, 184422 (2005).
[24] R. R. Urbano, P. G. Pagliuso, C. Rettori, S. B. Oseroff, J. L. Sarrao, P. Schlottmann, and Z. Fisk, Phys. Rev. B **70**, 140401(R) (2004).
[25] A. Abragam and B. Bleaney, EPR of Transition Ions (Clarendon Press, Oxford, 1970).
[26] G. E. Pake and E. M. Purcell, Phys. Rev. **74**, 1184 (1948).
N. Bloembergen, J. Appl. Phys. **23**, 1383 (1952).
G. Feher and A. F. Kip, Phys. Rev. **98**, 337 (1955).
F. J. Dyson, Phys. Rev. **98**, 349 (1955).
[27] J. W. Essam, in: Phase Transitions and Critical Phenomena, Vol. 2, edited by C. Domb and M. S. Green (Academic Press, London, 1972), p. 197.
P. Schlottmann and C. S. Hellberg, J. Appl. Phys. **79**, 6414 (1996).
[28] G. A. Wigger, C. Beeli, E. Felder, H. R. Ott, A. D. Bianchi, and Z. Fisk, Phys. Rev. Lett. **93**, 147203 (2004).